qualitatively predict the positive shift of $g_\perp$ that was observed.

One can also attempt to obtain information from the A values. We observed $A_{iso} = (A_\parallel + 2A_\perp)/3 = 25 \times 10^{-4}$ cm^{-1} and $A_{dip} = (A_\parallel - A_\perp)/3 = -1.67 \times 10^{-4}$ cm^{-1}. Norman et al.[5] have calculated A values by estimating spin polarization at the nucleus and report a value for A_{iso} of 9×10^{-4} cm^{-1}. A dipolar contribution of -0.6×10^{-4} cm^{-1} was also obtained. As these authors point out, these theoretical values are very crude. Ideally, inclusion of a very large number of higher order terms is needed, which would lead to greater electron spin density at the nucleus. The value reported here for $A_\parallel$ (21.7×10^{-4} cm^{-1}) is much different from the previously reported value ($9 (\pm 3) \times 10^{-4}$ cm^{-1}), which causes both A_{iso} and A_{dip} to be in much better agreement with the rough theoretical values.

Conclusions. $Ru_2(but)_4Cl$, a typical example of the ruthenium carboxylate dimer, was studied with use of variable-temperature powder magnetic susceptibility and frozen-solution EPR spectroscopy at 4 K. The complex is an $S = {}^3/_2$ system as was originally proposed.[8] In contrast to earlier suggestions,[4] there are no noticeable interdimer magnetic effects in spite of the polymeric solid-state structure of the complex. The complex does exhibit large zero-field splitting due to spin–orbit coupling. Electron spin density is delocalized over both Ru atoms as with other metal carboxylate dimer radicals. It is possible that the two Ru atoms are not exactly equal, but this difference cannot be resolved without isotopically pure Ru. Far-IR spectroscopy showed a previously unreported ν(RuCl) band. The experimental results provide support for the MO scheme of Norman et al.[5]

Acknowledgment. We thank the National Science Foundation for support of this research. The assistance of Mark Timken with the magnetic susceptibility programs and Jeffrey Cornelius with the EPR programs is gratefully acknowledged.

Registry No. $Ru_2(but)_4Cl$, 53370-31-3.

Contribution from the Departments of Chemistry, University of Florida, Gainesville, Florida 32611, and University of Illinois, Urbana, Illinois 61801

EPR Spectra and Bonding in the 2:1 Base Adducts of $Rh_2(carboxylate)_4^+$

RUSSELL S. DRAGO,* RICHARD COSMANO, and JOSHUA TELSER

Received January 10, 1984

In this paper, EPR studies are reported on a series of 1:1 and 2:1 adducts of $Rh_2(butyrate)_4^+$. The results provide a simplified interpretation of the EPR spectra of the 2:1 adducts. The key feature is the energy of the additional molecular orbital that arises when the donor lone pair is mixed into the 1:1 adduct to form the 2:1 adduct. When the donor lone pair ionization potential is low (C number is large) and the interaction strong, this σ molecular orbital becomes the HOMO and an EPR signal is detected. When the donor ionization potential is high and the interaction weak, the HOMO is π^* and no EPR spectrum is seen. The EPR spectrum of the cation provides no insight into the question of π-stabilization. Clearly, in the CO adducts the π-back-bonding is slight compared to that of most metal carbonyls but it is a significant fraction of the total weak interaction of CO with this acid. The complexes formed when pyridine or *N*-methylimidazole is added in excess to the radical cation do not have axial symmetry.

Introduction

There is considerable interest in metal-cluster chemistry, and the bimetallic carboxylate systems are among the most extensively studied of these. Numerous theoretical, structural, and reactivity studies of rhodium(II) carboxylates[1] have been reported. The nature of the metal–metal interaction in rhodium(II) carboxylates, as well as the electronic structure of their adducts, has been a source of controversy over the years. X-ray crystal structure results[2] and theoretical MO calculations[3] have often led to conflicting conclusions. Clearly, the energy differences of different electronic states are slight, and the results of calculations remain suspect. Different calculational methods give different results,[3] and all fail to account for all known properties For example, ab initio calculations[3d] lead to a HOMO that is σ in nature while an SCF–Xα–SW approach indicates[3c] it is δ^*. In an attempt to solve the problem in an experimental manner, we reported[4] in 1977 an EPR spectrum for the TMPNO adduct of rhodium trifluoroacetate. The results were interpreted in terms of the simplified MO model shown in Figure 1. The appearance of rhodium hyperfine interactions in the spectrum of the radical, as well as a sizable shift in the g value compared to that of the noncomplexed base, was taken as evidence that some type of π-interaction was occurring between the rhodium atom and the nitroxide radical base.

Calorimetric studies of rhodium(II) butyrate later showed[5] that there was a bonding interaction occurring between the metals and certain axial bases that could not be accounted for by a σ-only bond as viewed in the E and C model. Comparison of the enthalpies of adduct formation with the observed changes in the visible spectrum and the electrochemical behavior of the 1:1 adducts were consistent with the interpretation that the anomalous bonding interaction involved a back-donation of π^*-electron density from high-energy, rho-

* To whom correspondence should be addressed at the University of Florida.

(1) (a) Boyar, E. D.; Robinson, S. D. *Coord. Chem. Rev.* **1983**, *50*, 109 and references therein. (b) Cotton, F. A.; Walton, R. A. "Multiple Bonds Between Metal Atoms"; Wiley-Interscience: New York, 1982; and references therein. (c) Felthouse, T. R. *Prog. Inorg. Chem.* **1982**, *29*, 73 and references therein.

(2) (a) Christoph, G. G.; Halpern, J.; Khare, G. P.; Koh, Y. B.; Romanowski, C. *Inorg. Chem.* **1981**, *20*, 3029 and references therein. (b) Caulton, K. G.; Cotton, F. A. *J. Am. Chem. Soc.* **1971**, *93*, 1914 and references therein. (c) Bursten, B. E.; Cotton, F. A. *Inorg. Chem.* **1981**, *20*, 3042.

(3) (a) Dubicki, K.; Martin, R. L. *Inorg. Chem.* **1970**, *9*, 673. (b) Norman, J. G.; Kolari, H. J. *J. Am. Chem. Soc.* **1978**, *100*, 791. (c) Norman, J. G.; Renzoni, G. E.; Case, D. A. *J. Am. Chem. Soc.* **1979**, *101*, 5256. (d) Nakatsuji, H.; Onishi, Y.; Ushio, J.; Yonezawa, T. *Inorg. Chem.* **1983**, *22*, 1623.

(4) Richman, R. M.; Kuechler, T. C.; Tanner, S. P.; Drago, R. S. *J. Am. Chem. Soc.* **1977**, *99*, 1055.

(5) (a) Drago, R. S.; Tanner, S. P.; Richman, R. M.; Long, J. R. *J. Am. Chem. Soc.* **1979**, *101*, 2897. (b) Drago, R. S.; Long, J. R.; Cosmano, R. *Inorg. Chem.* **1981**, *20*, 2920. (c) Drago, R. S. *Inorg. Chem.* **1982**, *21*, 1697.

0020-1669/84/1323-3120$01.50/0

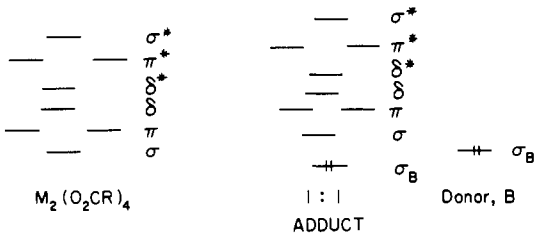

Figure 1. Simplified molecular orbital scheme for $M_2(carboxylate)_4$ compounds and their 1:1 donor adducts.

dium antibonding molecular orbitals to axial ligands capable of acting as π-acceptors. Later investigation[6] of the molybdenum(II) heptafluorobutyrate dimer, which lacks π^* electrons, showed that there was no corresponding bonding stabilization over and above that predicted for a σ-only bond between the acid and base. This finding further supports the interpretation that there is π-stabilization in the rhodium case and supports our model for explaining the cause of this stabilization from a synergistic metal–metal interaction.[5]

Other workers, however, have come to a different conclusion concerning the nature of the adduct bond for rhodium(II) carboxylates, specifically, that the interaction can be described solely in terms of a σ bond. EPR studies by Kawamura et al.[7] of the radical cations of $Rh_2(O_2CR)_4(PY_3)_2$ (where R = Et or CF_3 and PY_3 = PPh_3, $P(OPh)_3$, or $P(OCH_2)_3CEt$) were found to be consistent with the interpretation that the axial bond between the rhodium and phosphorus atoms consists of a σ bond with no indication of π-stabilization. Ab initio HF calculations and an SCF–Xα treatment of $Rh_2(O_2CH)_4(PH_3)_2$ were found[2c] to be consistent with the HOMO of the adduct having substantial contributions from both the rhodium and phosphorus atom σ orbitals.

The seeming contradiction of the thermodynamic evidence on the one hand and the EPR evidence on the other led to the decision to extend the EPR work on the rhodium dimer to include other conditions and bases. To that end, the EPR spectra of 1:1 and 2:1 adducts for a series of radical cations of rhodium butyrate with phosphorus, nitrogen, oxygen, and sulfur donors were investigated.

Most of the experimental results on various metal carboxylates and their 1:1 adducts are understood in terms of the simple molecular orbital diagram we reported in an earlier study (Figure 1). Though there is some question regarding the relative position of the δ^* and π^* orbitals, this d-orbital order can be used to rationalize bond distances and UV–visible and EPR spectra of the 1:1 adducts. As we shall show, most of the seeming contradictions arise from the inappropriate use of the 1:1 MO scheme to predict the HOMO for 2:1 adducts.

Experimental Section

A. Synthesis and Purification. 1. Metal Complexes. Tetrakis(acetato)dirhodium(II) is produced from $RhCl_3 \cdot 3H_2O$ according to the method of Wilkinson et al.[8] $RhCl_3 \cdot 3H_2O$ is dissolved in ethanol with NaO_2CCH_3 and CH_3CO_2H. The initial red solution changes to dark green upon refluxing for approximately 1 h. The green solid (crude rhodium acetate) that precipitates is then recrystallized from methanol, yielding the bluish green methanol adduct. Heating under vacuum overnight gives the pure emerald green rhodium acetate dimer. The acetate is then converted to the butyrate by refluxing the dimer in a solution of butyric acid and butyric anhydride (1 g:30 mL:2 mL) at about 100 °C and 150 torr for 3 h under a nitrogen atmosphere. The volume is then reduced by 80%, and the solution is left at −20 °C overnight. The solid is filtered off, washed with cold pentane, and dissolved in hot benzene; the mixture is filtered and concentrated to 5 mL. After cooling, $Rh_2(But)_4$ (But = butyrate) crystallizes and is filtered, washed with cold pentane, and heated in vacuo over NaOH overnight.

Anal. Calcd for $Rh_2C_{16}H_{28}O_8$: C, 34.67; H, 5.10. Found: C, 34.56; H, 5.20.

The bis(triphenylphosphine) adduct of rhodium butyrate is synthesized by mixing $Rh_2(But)_4$ with exactly 2 equiv of PPh_3 in CH_2Cl_2, followed by evaporation of the solvent. Excess triphenylphosphine cannot be removed easily from the solid product if more than a 2:1 ratio of base to acid is used.

Anal. Calcd for $Rh_2C_{52}H_{58}O_8P_2$: C, 57.89; H, 5.43; P, 5.74. Found: C, 58.07; H, 5.51; P, 5.88.

2:1 and 1:1 adducts of $Rh_2(But)_4$ with *N*-methylimidazole, pyridine, acetonitrile, tetrahydrothiophene (THTP), dimethyl sulfoxide, pyridine *N*-oxide, methanol, and carbon monoxide were not isolated but were generated in solution directly by addition of stoichiometric amounts of base (except for CO, which was bubbled through) to CH_2Cl_2 solutions of $Rh_2(But)_4$, leading to the characteristic color[1,5] of the adducts. These adducts have been previously studied quantitatively in solution.[5,6] Furthermore, solid 2:1 adducts of $Rh_2(O_2CCH_3)_4$ with all of the above bases except pyridine *N*-oxide have been reported.[1]

2. Bases. Standard literature procedures were used to purify and dry the bases used in these studies.[9] All bases were obtained as reagent grade quality chemicals. Pyridine is stored over KOH until needed, at which time it is fractionally distilled from BaO. Acetonitrile is stirred over CaH_2 for 24 h and then fractionally distilled from phosphorus(V) oxide. *N*-Methylimidazole (*N*-MeIm) is stirred over KOH for 24 h and fractionally distilled at reduced pressure from CaH_2. Dimethyl sulfoxide is stored for 24 h or more over NaOH and fractionally distilled from fresh NaOH at reduced pressure. 4-Picoline *N*-oxide is recrystallized in an ethanol/ether solution and then sublimed twice at 1 torr and 70 °C. Tetrahydrothiophene (THTP) is fractionally distilled from CaH_2. The first and last fractions for any of the above distillations are discarded, and all liquids are stored over 4A molecular sieves.

3. Solvents. Bulk methylene chloride was washed twice with sulfuric acid for $^1/_2$ day each time, followed by washes with aqueous carbonate and water.[9] It was then stored for at least 24 h over calcium chloride. This predried solvent can then be distilled from phosphorus(V) oxide and stored over 4A sieves. When reagent grade CH_2Cl_2 is used, the prewash can be omitted.

4. Electrolyte. Tetra-*n*-butylammonium tetrafluoroborate was prepared according to literature methods.[10]

Anal. Calcd for $C_{16}H_{36}NBF_4$: C, 58.35; H, 11.04; N, 4.25. Found: C, 58.39; H, 11.07; N, 4.26.

B. Apparatus. Cyclic voltammetry experiments were performed by using a standard three-electrode arrangement. A platinum disk served as the working electrode, while a platinum wire was used as the counterelectrode. The reference electrode consisted of a silver wire suspended in a saturated AgI solution of CH_2Cl_2 that was 0.42 M in Bu_4NBF_4 and 0.05 M in Bu_4NI. All electrolyte solutions were 0.42 M Bu_4NBF_4 in CH_2Cl_2. Sample solutions were contained in a sealed cell that was purged and maintained under an Ar atmosphere. A PAR Model 173 potentiostat/galvanostat and Model 176 current-to-voltage converter were then used to generate the voltammograms on an X-Y recorder.

Generation of the radicals for EPR was accomplished by the use of a specially designed cell. The cell also used the standard three-electrode configuration. The reference electrode and counterelectrode were contained in a reservoir attached to the top of an EPR tube with the working electrode (a platinum wire) extending down the length of the EPR tube. The applied potential was then maintained at 150–250 mV more positive than the $E_{1/2}$ of the redox couple involved, and the EPR signal was monitored continually with time. Characteristic color changes that might occur upon the production of a radical in solution could then be followed in the reservoir above. the EPR spectra were obtained on a Varian E-9 X-band spectrometer.

(6) Drago, R. S.; Long, J. R.; Cosmano, R. *Inorg. Chem.* **1982**, *21*, 2196.
(7) (a) Kawamura, T.; Fukamachi, K.; Hayashida, S. *J. Chem. Soc., Chem. Commun.* **1979**, 945. (b) Kawamura, T.; Fukamachi, K.; Sowa, T.; Hayashida, S.; Yonezawa, T. *J. Am. Chem. Soc.* **1981**, *103*, 364. (c) Sowa, T.; Kawamura, T.; Shida, T.; Yonezawa, T. *Inorg. Chem.* **1983**, *22*, 56.
(8) (a) Legzdins, P.; Mitchell, R. W.; Rempel, G. L.; Ruddick, J. D.; Wilkinson, G. *J. Chem. Soc. A* **1970**, 3322. (b) Rempel, G. L.; Legzdins, P.; Smith, H.; Wilkinson, G. *Inorg. Synth.* **1971**, *13*, 90.
(9) (a) Gordon, A. J.; Ford, R. A. "The Chemist's Companion"; Wiley: New York, 1972. (b) Long, J. R. Ph.D. Thesis, University of Illinois, 1980.
(10) Richman, R. M. Ph.D. Thesis, University of Illinois, 1976.

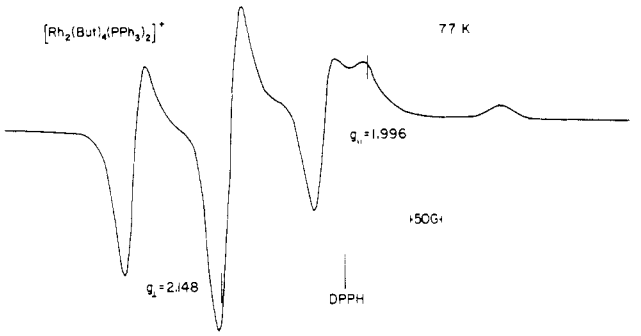

Figure 2. EPR spectrum of the 2:1 triphenylphosphine adduct of $Rh_2(But)_4^+$.

Computer simulations of EPR spectra were performed with an EPR powder pattern simulation program.

Results and Discussion

Some aspects of the thermodynamic and electrochemical behavior of rhodium butyrate and its adducts have been reported previously. $Rh_2(But)_4$ is capable of reacting with a wide range of bases that include a number of different donor atoms. As the earlier results indicated,[5] some of the axial bases appeared to act as acceptors for metal π^*-electron density; that is, in certain instances the bonding interaction was enhanced by a π-stabilization involving the donation of metal electron density into orbitals in the bases capable of overlapping with the π^* orbitals of the dimer. Caged phosphite, $P(OCH_2)_3CEt$, was one such base that appeared to undergo a π-interaction with the rhodium dimer. It was determined that, of a total enthalpy of 16.8 kcal mol^{-1} for the formation of the 1:1 adduct, 6.6 kcal mol^{-1} could not be accounted for by a σ-only interaction and thus resulted from π-stabilization. The generalization of this finding provides an important mechanism for predicting synergism in metal–metal bonding.[5] The conclusion by Kawamura et al.,[7] that there was no π-interaction in the adduct of rhodium propionate with caged phosphite on the basis of their EPR spectra was therefore both interesting and unexpected.

To demonstrate that there would be no difference between the radical-cation EPR spectra of rhodium butyrate and rhodium propionate, the 2:1 PPh_3 adduct of $Rh_2(But)_4$ was electrochemically oxidized at +1.1 V vs. Ag/Ag^+ ($E_{1/2}$(2:1) = 0.90 V vs. Ag/Ag^+) and the EPR spectrum at liquid-nitrogen temperature was recorded (Figure 2). It agrees quite well with that reported by Kawamura for the propionate.[7] Simulation of the spectrum gives g values and hyperfine constants that agree with those reported in the literature.[7] There are some important features of the spectrum to note, upon which the σ-only bonding arguments were made. The first point is that $g_\perp$ (2.148) is greater than $g_\parallel$ (1.996). If the unpaired electron in the radical cation were in fact in a π^* orbital of the rhodium dimer, one might expect a fair amount of spin–orbit coupling to occur due to the degeneracy of these π^* orbitals (Figure 1). Assuming $g_\parallel$ to lie along the Rh–Rh bond would lead to $g_\parallel > g_\perp$. This is opposite from that found by experiment. The g values are more consistent with the unpaired electron being in an orbital of σ symmetry. In this case, $g_\parallel$ would be expected to be close to the free-electron value (2.0023) because of minimal spin–orbit coupling, and $g_\perp$ would be greater than both $g_\parallel$ and g_e due to matrix elements mixing in the degenerate rhodium π orbitals.

The large phosphorus hyperfine interaction, corresponding to a total of 53% of the electron density being on the phorphorus atoms, is also consistent with the unpaired electron being in an orbital with large phosphorus s and p_z orbital contributions rather than in rhodium π^* orbitals. In addition, the assignment of the unpaired electron to an orbital with a large phosphorus component and σ symmetry with respect to the P–Rh–Rh–P axis is suggested by the fact that $A_\parallel$(P) is greater than $A_\perp$(P). The possibility that the spectrum is simply due to an unpaired electron in a phosphorus lone-pair orbital can be dismissed since there is a rhodium contribution to the hyperfine interaction and $g_\perp$ is greater than what would be expected for a phosphorus radical.

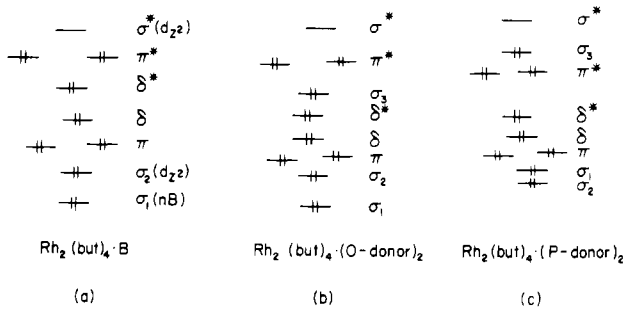

Figure 3. Simplified molecular orbital diagram relating the 1:1 and 2:1 adducts of $Rh_2(But)_4$: (a) 1:1 adduct and (b) 2:1 adduct with a π^* HOMO; (c) 2:1 adduct with a σ_3 HOMO.

Kawamura et al.[7] conclude that the strong σ-type interaction between the rhodium and phosphorus atoms would be expected to drastically alter the ground-state electronic configuration of the dimer, making a σ or σ^* orbital higher in energy than the π^* orbitals; therefore, there is no reason to invoke a π-interaction between the metal and base to lower π^*.

Our view of the bonding in these adducts is consistent with these EPR results and also with the π-stabilization inferred from other studies. The key is to view the 1:1 adduct σ system as a three-center bond giving rise to σ_1 (nB = base lone pair), σ_2 (metal d_{z^2}) and σ^* (metal d_{z^2}) MO's as shown in Figure 3 with the symbol in parentheses indicating the principal AO contributor. However, the 2:1 adduct must now be treated as a four-center σ system, and the important feature is the location of the additional molecular orbital, σ_3, arising from mixing in the lone-pair orbital of the second donor. When the donor orbital energy is low and the interaction of weak or moderate strength, this new molecular orbital (σ_3) will lie below π^* and the HOMO will be π^*. This situation is illustrated in Figure 3b. When the donor orbital energy is high and the interaction moderate or strong, the HOMO will be σ_3 as shown in Figure 3c. The existence of π^* to ligand back-bonding will decrease the energy of π^*, increasing the σ_3–π^* gap in the case shown in Figure 3c and decreasing the gap or even reversing the order of σ_3 and π^* in the case illustrated in Figure 3b. Thus, the HOMO in the radical cation formed from the 2:1 adduct provides no insight into the question of π-back-bonding unless a reversal is observed.

When the phosphorus donor concentration is varied, the change in the HOMO on going from the 1:1 to 2:1 adduct can be dramatically shown by EPR. Figure 4 shows the cyclic voltammograms for the free acid and 1:1 and 2:1 phosphine:acid ratios along with the corresponding EPR spectrum. As the amount of 2:1 adduct in the system is decreased (observe the decreasing size of the wave on the right in the voltammogram), the intensity of the EPR signal diminishes. At concentrations of PPh_3 where almost no 2:1 adduct exists and the predominant adduct is 1:1, no EPR signal is observed. Thus the 1:1 and 2:1 adducts have very different EPR behavior, which is what would be expected by comparison of their MO schemes (Figure 3a,c). In the 2:1 adduct the electron is in a singly degenerate orbital of axial symmetry. In the 1:1 adduct it is in a doubly degenerate orbital as it is in the $Rh_2(But)_4^+$ radical cation. The doubly degenerate π^* orbital allows for a great deal of spin–orbit coupling, and no EPR signal is observed at liquid-nitrogen temperatures, 77 K.

The radical cation of the known 2:1 adducts of the weak donors, pyridine *N*-oxide, acetonitrile, tetrahydrothiophene,

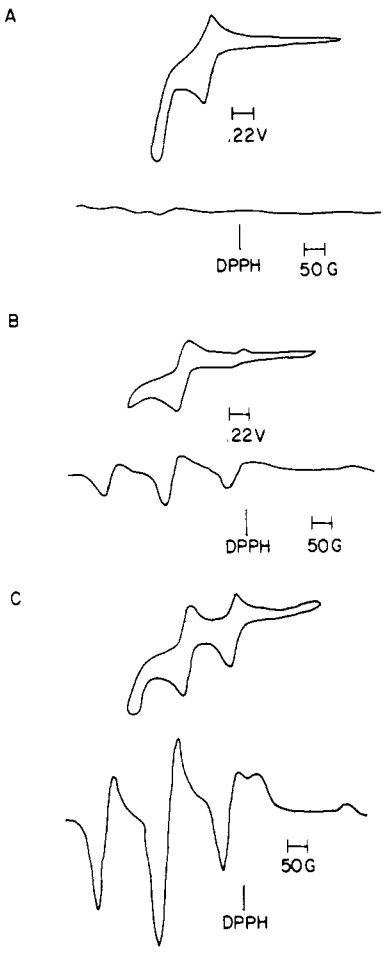

Figure 4. Voltammograms and corresponding EPR spectra of oxidized complexes at varying concentrations of triphenylphosphine: (a) free acid; (b) 1:1 phosphine:$Rh_2(But)_4$ ratio; (c) 2:1 phosphine:$Rh_2(But)_4$ ratio.

dimethyl sulfoxide, and methanol, were not observed by EPR. Since these weak donors consist of systems capable of both σ-only and σ–π bonding, we can conclude that the strength of the acid–base interaction rather than the type of bonding involved is important in deciding whether or not an EPR spectrum is observed at liquid-nitrogen temperatures in the systems studied. Our inability to see an EPR signal at 77 K can be rationalized with the simplified model. The lower energy, weaker donor orbitals of these ligands lead to adducts in which the HOMO is the π^* orbtial as shown in Figure 3b. With the π^* orbitals highest in these cation adducts, larger spin–orbit coupling is expected than for electron occupancy in a singly degenerate orbital, leading to more efficient relaxation of the electron spin and no observable EPR signal. This explanation receives support from the observation that an EPR spectrum is not observed at liquid-nitrogen temperatures for the cation radical generated from the free acid. The systems investigated in this study are summarized in Table I, and it can be seen than the results are consistent with this model. No evidence for or against the π-stabilization observed in the calorimetric studies can be obtained from EPR. Similar complications arise in inferring π-back-bonding[7] from infrared studies of the CO adduct. It should be emphasized that binding of CO by $Rh_2(carboxylate)_4$ is very weak. Thus the high frequency of the CO stretch does not, as reported,[7c] indicate the absence of π-stabilization. A considerable fraction of the weak interaction could be from π-stabilization, but the perturbation from σ effects could cause an increase in the ν_{CO} force constant comparable to the decrease caused by π effects in this region of weak interaction. If BF_3, a σ-only acid with

Table I. EPR Detection and $E_{1/2}$ for Donor Adducts of $Rh_2(But)_4^+$

donors	EPR signal obsd	$E_{1/2}$, V
2:1 PPh_3	yes; $g_\parallel = 1.996$, $g_\perp = 2.148$; $A_\parallel(P) = 203 \times 10^{-4}$ cm^{-1}, $A_\perp(P) = 152 \times 10^{-4}$ cm^{-1}, $A(Rh) = 13 \times 10^{-4}$ cm^{-1}	0.90
1:1 PPh_3	no	1.4
2:1 *N*-MeIm	yes; $g_x = 1.997$, $g_y = 2.017$, $g_z = 2.091$	1.04
1:1 *N*-MeIm	no	1.37
2:1 pyridine	yes	1.20
1:1 pyridine	no	1.45
2:1 acetonitrile	no	1.54
2:1 THTP	no	1.28
2:1 dimethyl sulfoxide	no	1.31
2:1 pyridine *N*-oxide	no	(1.3)[a]
2:1 methanol	no	1.37
2:1 CO	no	1.62
free acid	no	1.55

[a] $E_{1/2}$ is for the 1:1 adduct.

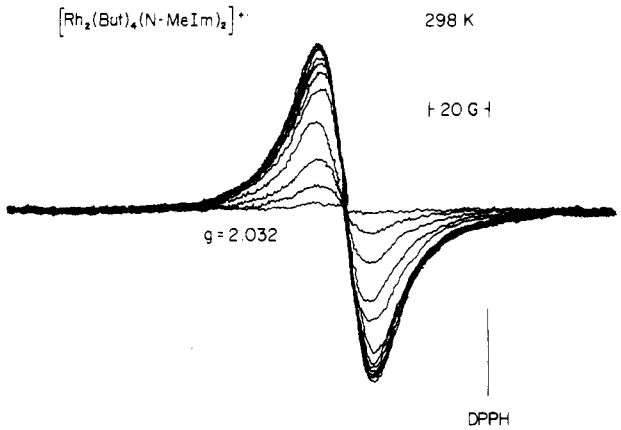

Figure 5. Room-temperature EPR spectra of $[Rh_2(But)_4(N\text{-MeIm})_2]^+$ as a function of time of electrochemical generation.

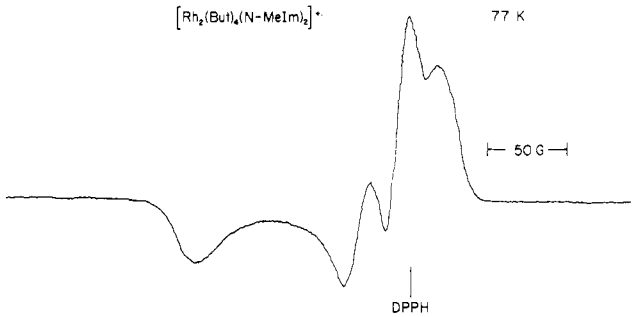

Figure 6. EPR spectrum of $[Rh_2(But)_4(N\text{-MeIm})_2]^+$ at liquid-nitrogen temperature.

greater E and C numbers than those of $Rh_2(carboxylate)_4$, does not bind CO, then π-stabilization is the expected cause of the additional stabilization that leads to CO complexation in the latter case.[5c] Although calorimetric studies have shown that there is π-back-bonding in some of these adducts, there apparently is not enough to lead to a reversal of the π^* and σ_3 orbitals (Figure 3b), which would allow observation of an EPR spectrum. Clearly, the π-back-bonding is small compared to that of many metal carbonyls, but it is significant compared to the metal–ligand σ interaction in these adducts.

The EPR spectra obtained for the radical cations in excess *N*-methylimidazole and excess pyridine are in sharp contrast to the results for the bis(phosphorus) adducts. The room-temperature spectrum of the former consists of a single broad resonance. The spectra as a function of time during electrolysis are shown in Figure 5. When the spectrum reached the

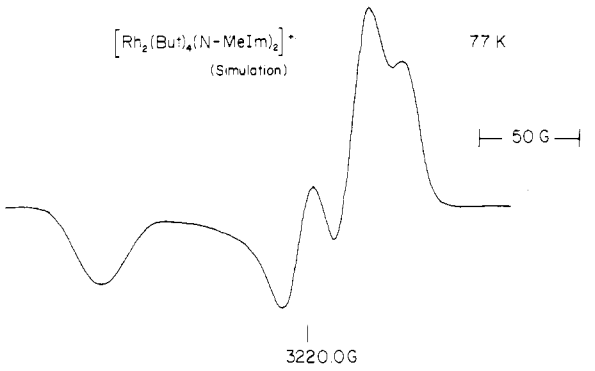

Figure 7. Simulation of the EPR spectrum of $[Rh_2(But)_4(N\text{-}MeIm)_2]^+$.

maximum intensity shown, the sample was lowered to liquid-nitrogen temperature. The 77 K spectrum is shown in Figure 6. Unlike the phosphorus case, the spectrum contains three *g* values. Simulation for the *N*-methylimidazole compound gives $g_x = 1.997$, $g_y = 2.017$, and $g_z = 2.091$. The simulated spectrum is shown in Figure 7. The rhodium and/or nitrogen hyperfine interactions are unresolved. Similar results were obtained with pyridine.

The three-*g*-value spectrum conclusively shows that the *N*-methylimidazole adduct does not have axial symmetry. It is clear that the highest lying orbital is not similar to that found for the bis(phosphorus) complex. Both pyridine (a π-interacting base) and *N*-MeIm (a non-π-interacting base) give three-*g*-value spectra as opposed to the axial spectra of the phosphorus bases. We suspect that the species formed in the case of pyridine and *N*-methylimidazole have monodentate butyrate with the vacated coordination sites occupied by these donors. Only by disrupting the bridging carboxylate framework can there be such a decidedly nonaxial system. There is precedence for this type of reaction for rhodium trifluoroacetate.[12]

Acknowledgment. The authors acknowledge partial support of this research by the National Science Foundation.

(11) The program is titled QPOW and was obtained from R. L. Belford at the University of Illinois and modified by M. Kroeger and K. Leslie.
(12) Telser, J.; Drago, R. S. *Inorg. Chem.* **1984**, *23*, 2599.

Contribution from the School of Chemical Sciences, University of Illinois, Urbana, Illinois 61801, and Department of Chemistry, University of Delaware, Newark, Delaware 19711

$Cu_2(o\text{-}Ph_2PC_6H_4C(O)CHC(O)C(CH_3)_3)_2$: Synthesis, Structure, and Ligand Oxygenation to a Mixed-Valence Cu(I)–Cu(II) Complex

DEBRA A. WROBLESKI,[1a] THOMAS B. RAUCHFUSS,*[1a] ARNOLD L. RHEINGOLD,*[1b] and KEITH A. LEWIS[1b]

Received October 18, 1983

The synthesis of (*o*-(diphenylphosphino)benzoyl)pinacolone (HacacP) is described. The complexes $M_2(acacP)_2$ (M = Cu, Ag) were synthesized from the reaction of HacacP, NEt_3, and $Cu(CH_3CN)_4ClO_4$ or $AgClO_4$. Treatment of a CH_2Cl_2 solution of $Cu_2(acacP)_2$ (**1**) with molecular oxygen gave $Cu_2(acacP)_2(\mu\text{-}o\text{-}O_2CC_6H_4P(O)Ph_2)$ (**2**), which can also be prepared by treatment of **1** with $Cu(o\text{-}Ph_2P(O)C_6H_4CO_2)_2$ and HacacP. After demetalation the organic products of the oxygenation were found to consist of equal amounts of $o\text{-}Ph_2P(O)C_6H_4CO_2H$ and $t\text{-}BuCO_2H$, which were derived from $acacP^-$. The crystal structure and molecular geometry of $Cu_2(acacP)_2(o\text{-}O_2CC_6H_4P(O)Ph_2)$ has been determined by X-ray diffraction: $P\bar{1}$, $a = 13.592$ (4) Å, $b = 14.913$ (5) Å, $c = 18.501$ (5) Å, $\alpha = 85.78$ (3)°, $\beta = 86.19$ (2)°, $\gamma = 72.61$ (2)°, $Z = 2$, $\mu = 7.17$ cm^{-1} (Mo Kα). The crystal structure and molecular geometry of $[Cu(acacP(O))(OCH_3)]_2\cdot 2CH_3OH$ have been determined by X-ray diffraction: $P2_1/n$, $a = 9.750$ (2) Å, $b = 16.399$ (3) Å, $c = 16.698$ (4) Å, $\beta = 97.25$ (2)°, $Z = 2$, $\mu = 9.17$ cm^{-1} (Mo Kα).

Introduction

The rarity of bimetallic coordination compounds where *both* metals are reactive contrasts sharply with the variety of bimetallic complexes that are chemically dormant.[2] In recent years this deficiency has been addressed through reactivity studies on A-frame complexes of bis(phosphine) ligands[3] and complexes of face-to-face porphyrins.[4] Our contribution to this area follows from work with the "compartmentalized" phosphine β-diketone, (*o*-(diphenylphosphino)benzoyl)pinacolone, HacacP.[5]

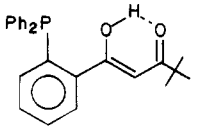

As expected for a ligand of its complexity, $acacP^-$ can bind two metals in a variety of ways. The simplest and, structurally, the most unusual of its bimetallic derivatives is $Cu_2(acacP)_2$ (**1**), which consists of two cofacially arrayed 3-coordinate copper(I) centers (Figure 1). Compound **1** has a rich chemistry: it undergoes 1-electron oxidative addition,[6] it reversibly binds *o*-quinones,[7] and it reacts readily with molecular oxygen. In this report we describe the preparation of HacacP, **1**, and the products formed upon oxygenation of **1**. Copper-catalyzed substrate oxygenation is an important biochemical process,[8] and it is only very recently that Karlin,[9] Rogić,[10] and others have demonstrated the hydroxylation of an aromatic ring through studies on synthetic complexes.

(1) (a) University of Illinois. (b) University of Delaware.
(2) Groh, S. E. *Isr. J. Chem.* **1976/77**, *15*, 277.
(3) Kubiak, C. P.; Woodcock, C.; Eisenberg, R. *Inorg. Chem.* **1982**, *21*, 2119.
(4) Collman, J. P.; Chong, A. O.; Jameson, G. B.; Oakley, R. T.; Rose, E.; Schmittou, E. R.; Ibers, J. A. *J. Am. Chem. Soc.* **1981**, *103*, 516.
(5) Rauchfuss, T. B.; Wilson, S. R.; Wrobleski, D. A. *J. Am. Chem. Soc.* **1981**, *103*, 6769.
(6) Wrobleski, D. A.; Wilson, S. R. Rauchfuss, T. B. *Inorg. Chem.* **1982**, *21*, 2114.
(7) Rauchfuss, T. B., unpublished results.
(8) Ibers, J. A.; Holm, R. H. *Science* (*Washington, D.C.*) **1980**, *209*, 223.
(9) (a) Karlin, K. D.; Dahlstrom, P. L.; Cozzette, S. N.; Scensny, P. M.; Zubieta, J. *J. Chem. Soc., Chem. Commun.* **1981**, 881. (b) Karlin, K. D.; Gultneh, Y.; Hutchinson, J. P.; Zubieta, J. *J. Am. Chem. Soc.* **1982**, *104*, 5240.
(10) Demmin, T. R.; Swerdloff, M. D.; Rogić, M. M. *J. Am. Chem. Soc.* **1981**, *103*, 5795 and references therein.

0020-1669/84/1323-3124$01.50/0